Construction of a Prediction Model for the Time Series of Brain Strain of a Novel Head Surrogate Using Deep Learning

Shuntaro Tamai
Yusuke Miyazaki
Hiroki Yamamoto
Tokyo Institute of Technology
Japan
Katsushi Yoshii
Ichiro Amamori
Joyson Safety Systems Japan
Japan

Paper Number 23-0239

ABSTRACT
An effective brain injury risk assessment is required to minimize the risk of brain injury from traffic accidents. Thus, anthropomorphic test devices (ATD) have been used for overall vehicle safety evaluation. We developed a novel ATD head that incorporates detailed intracranial structures with the brain and can measure the relative displacement between the brain and the skull. However, the strain inside the deep brain of the head surrogate cannot be measured or estimated. Although we can simulate the brain strain waveform using the finite element model, the computational cost is high, and the real-time evaluation of brain strain during crash tests is difficult. To compute the brain strain response in real-time, deep learning (DL) methods can be used to predict brain strain behavior. Therefore, this study aims to propose a method to predict the waveforms of maximum principal strain in the brain using a DL method called long short-term memory (LSTM). Reconstructed simulations for impact tests using a finite element head model were conducted to obtain the principal strain waveforms of the brain and construct a dataset for machine learning. The impact tests included 125 occipital head impact tests, 7 frontal sled tests, 35 vehicle frontal crash tests, and 53 American football impact tests, constituting a total of 220 head impact tests. Furthermore, the LSTM model was trained on triaxial angular velocity and acceleration waveforms, and the models were constructed to predict the principal strain waveforms in the cerebellum, brainstem, and right and left cerebrums. Subsequently, to validate the predictive model of brain strain, CORA was calculated as an index of the prediction error. The average CORA score between the brain strain waveforms predicted by LSTM and those of the dataset was 0.963 for occipital head impact tests, 0.928 for frontal sled tests, 0.898 for vehicle frontal crash tests, and 0.875 for American football tests. The occipital head impact tests, vehicle frontal crash tests, and frontal sled test cases were predicted with high accuracy. However, the football impact test cases were inferior to the other three test cases. The football impact cases included more multidirectional impact patterns and failed to learn similar collisions. However, an error in the waveform was observed in the rebound phase of the head impact in the latter half of the brain strain waveform. Therefore, the impact test dataset should be expanded, including cases with rebound behavior of the head, and the set of features that can reflect the rebound behavior of the head should also be examined further. In conclusion, the maximum principal strain waveforms of the brain can be rapidly and accurately predicted from the angular acceleration and angular velocity of the ATD head in occipital head impact, frontal sled, and vehicle crash test cases using LSTM. This method enables real-time evaluation of brain strain waveforms during impact tests.

INTRODUCTION

The number of fatalities from traffic accidents in Japan has been decreasing, but it remains high, accounting for over 40% of all injuries [1]. A more effective assessment of the brain injury risk is required to minimize the risk of brain injury due to accidents. Although we cannot directly measure the principal strain in the brain, which is a factor in the occurrence of brain

damage, we can simulate the deformation behavior of the human brain using finite element analysis (FEA). Therefore, integrating the calculation of brain deformation behavior using a human finite-element model with crash dummies can provide an injury evaluation function based on brain strain indices in crash tests. However, the FEA has computational costs, and real-time evaluation during crash tests is difficult. Therefore, developing a method that can minimize the computational cost while maintaining computational accuracy is necessary to obtain brain deformation behavior in real time. Wu et al. [2] applied a convolutional neural network (CNN) to estimate the 95% maximum principal strain (95%MPS) in the brain from entire-brain images. However, the output data are static and not time-series data.
This study aims to propose a fast and simple method for predicting the time-series waveform of the principal strain in the brain using long short-term memory (LSTM) and bidirectional LSTM with triaxial angular velocity and acceleration waveforms as an alternative to FEA. First, the 95%MPS in the brain induced by a head impact was calculated using FEA, and then, a model was constructed to predict the 95%MPS in the brain using LSTM by learning with triaxial angular velocity and angular acceleration waveforms. For training, we used head impact data obtained from occipital head impact tests [3], frontal sled tests [4], vehicle crash tests [5], and reconstruction tests of American football accidents [6][7]. The results show that LSTM and bidirectional LSTM quickly predict time-series waveforms.

METHODS

A flowchart of the study is shown in Figure 1. First, using the angular velocities of the three axes of the head obtained from various head impact tests as inputs, we conducted simulations using a finite element model of the head to obtain 95%MPS waveforms and constructed a dataset for deep learning. The deep learning model was then trained on the training dataset after appropriate pre-processing, and its performance was evaluated.

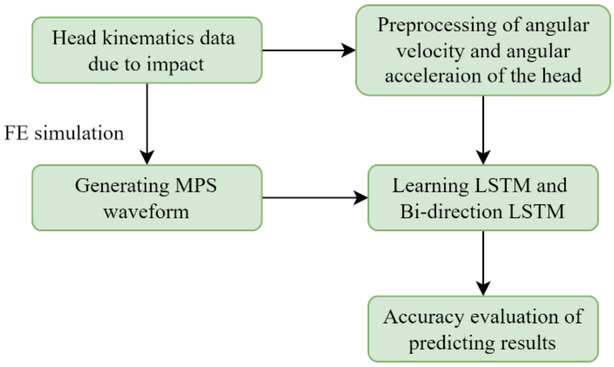

Figure 1. Flowchart

Data Description

The dataset used for training consisted of head impact data obtained from four tests: occipital head impact tests, frontal sled tests, vehicle crash tests, and reconstruction tests of American football collisions. An overview of these tests is provided below:

<u>Occipital Head Impact Tests</u>

The dataset of reconstruction tests of Depretiere's cadaver test was used [3]. Hybrid III AM50 with a novel anthropomorphic dummy head was used. An impactor (15.6 kg) was placed on the back of the dummy's head. The results of 125 occipital head impact tests obtained by varying the mass and velocity of the impactor were used.

<u>Frontal Sled Tests</u>

The dataset from frontal sled tests was used; a total of seven tests were used, varying the TTF of the delta-V and restraint system, using a full-body dummy with the head of the Hybrid III AM50 dummy replaced by a novel anthropomorphic dummy head [4]. Seven simulations were conducted.

Vehicle Crash Tests

Head motion data obtained from vehicle crash tests in the United States New Car Assessment Program were used. The three crash modes used in the simulations were the full-lap rigid barrier (FRB), left oblique impact (LOI), and right oblique impact (ROI). The simulations were performed on 35 cases: 6 FRB cases, 19 LOI cases, and 10 ROI cases.

Reconstruction tests head collision in American football

Head motion data were obtained from the head impact reconstruction test in American football conducted by Sanchez et al. [7]. In this experiment, the head impact position, angle, and velocity were estimated from the head impact video of American football games, and a Hybrid III dummy head wearing a helmet was used to reproduce the head impact situation. In total, 53 simulations were performed.

Finite Element Analysis

The head finite element model used in the simulation was constructed based on medical images of an adult male, as shown in Figure 2 [4]. The head finite-element model consists of the skin, skull, brain, meninges, venous sinus, cerebrospinal fluid, and ventricles. The skull has a cortical membrane and a trabecular body. The brain is modeled as a viscoelastic body using Maxwell–Kelvin viscoelastic material and consists of the right brain, left brain, cerebellum, and brain stem. The meninges were modeled as elastic bodies with the dura mater, soft membrane, cerebellar tent, and cerebral sickle. Cerebrospinal fluid, ventricles, and venous sinuses were modeled as fluids. The skull and skin of the model were made rigid, and simulations were conducted using the 6-axis motion data of the head in the various head impacts described above as inputs. The simulation output was the time-history waveforms of the 95th percentile maximum principal strain in the left and right cerebrum, brainstem, and cerebellum. LS-DYNA R11.1 was used as the solver.

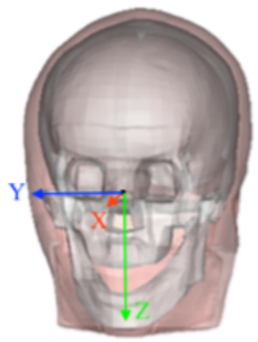

Figure 2. Entire structure of the FE head model and the head coordinate system

Feature Engineering and Data Preprocessing

A total of 31 features of the following four types obtained from the triaxial angular velocity waveforms were used as model inputs (Figure 3).

(1) Triaxial angular velocity ($\omega x,\ \omega y,\ \omega z$)

(2) Angular acceleration in each of the three axes ($\alpha x, \alpha y, \alpha z$)

(3) Absolute angular velocity ($|\omega|$)

(4) Angular velocity change ($\Delta\omega x, \Delta\omega y, \Delta\omega z, \Delta|\omega|$).

The angular velocity change is the magnitude of the change in angular velocity over T ms, calculated in Eq. 1 from the angular velocity and absolute value of angular velocity in the three axes. Six types of T were used (5, 10, 20, 30, 40, and 50), resulting in 24 features.

$$\begin{aligned} \Delta\omega(t) &= \omega(t) - \omega(T) \quad (T \le t) \\ \Delta\omega(t) &= \omega(t) \qquad\qquad\quad (T > t) \end{aligned} \qquad \text{Equation (1)}$$

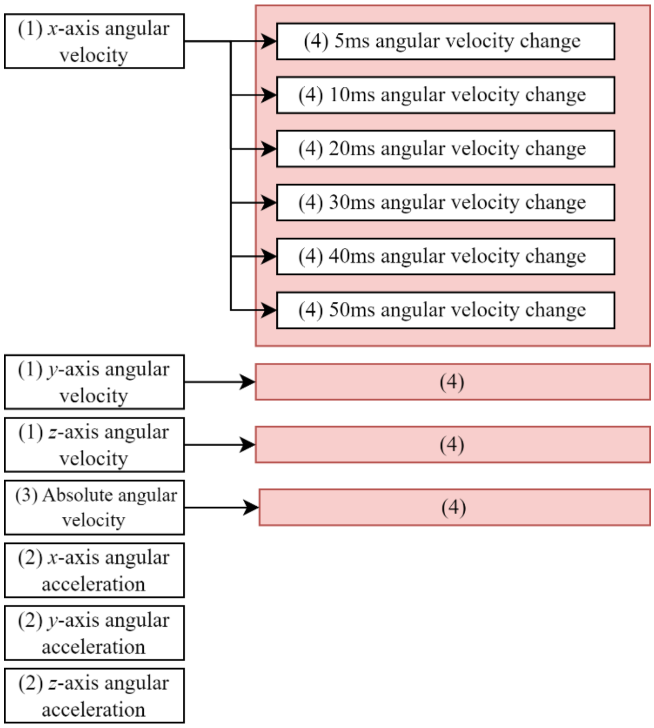

Figure 3. Overview of the input features

After feature engineering, the data were converted into a 31-column matrix for standardization and data augmentation. For data augmentation, the following two methods were applied to the training dataset.
(1) Inverted motions were created for each of the x- and z-axes to quadruple the dataset.
(2) The dataset was doubled by creating randomly scaled data at $0.9 \leq rate \leq 1.1$ for all features as input and all brain strain as output.
Finally, the total number of impact datasets is 1760 (220×4×2).

Deep Learning Model and Assessment

The head impact dataset was split into 80% training and 20% test data. The training data were inputted into a deep-learning model for training. The prediction error between the predicted and simulated principal brain strain waveforms was calculated for validation data. Accuracy was verified using the five-fold cross-validation method shown in Figure 4. In this study, LSTM and bidirectional LSTM were used as deep learning models.

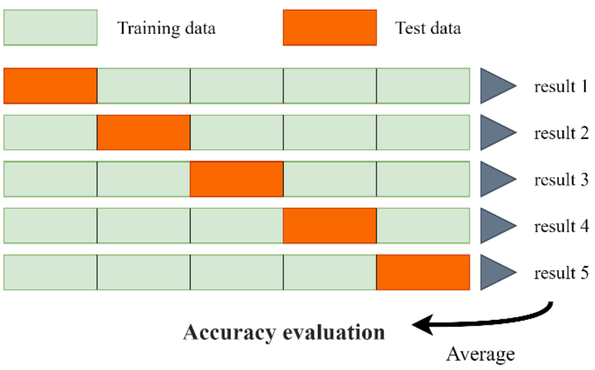

Figure 4. Fivefold cross-validation

LSTM Structure

LSTM is a network with a long-term dependency structure within the recurrent neural network (RNN). LSTM was proposed to address the long-term dependence [8][9]. In LSTM (Figure 5), the memory layer $\boldsymbol{C}^{(t)}$, which plays the role of long-term memory, is added from the RNN. After selecting the input information at the forgetting gate (f), the information is stored in the memory layer, and the next time step inherits the information from the memory layer. The information stored in the memory layer was transformed by an activation function and used to compute the output. The addition of this addresses the gradient loss problem.

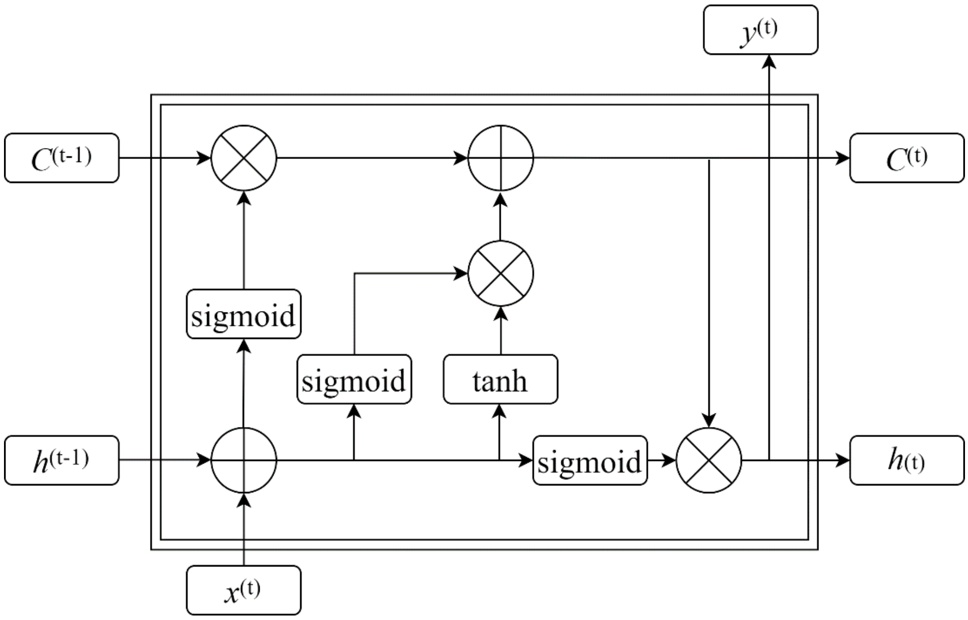

Figure 5. LSTM cell structure

The LSTM structure used in this study consists of five layers. (1) Input layer (31 units), (2) masking layer, (3) hidden layer (200 units, dropout: 0.2), (4) time-distributed layer with linear activation function, and (5) output layer (1 unit). Using the mean squared error as the loss function and adaptive moment estimation optimizer as the optimization function, the batch size was increased to 200-time steps to improve learning efficiency. The initial learning rate was set to 0.0004 and halved every two epochs for a total of six epochs.

Bi-directional LSTM Structure

Bi-directional LSTM [10] combines LSTM in the forward direction and LSTM in the reverse direction in a time series, as shown in Figure 6. The data used to construct the prediction model for the time-series waveform of brain strain can also be used to predict the data after the desired prediction. Therefore, we could make predictions in the reverse direction of a time series. Using both past and future information to predict a certain point in time is effective in improving accuracy.

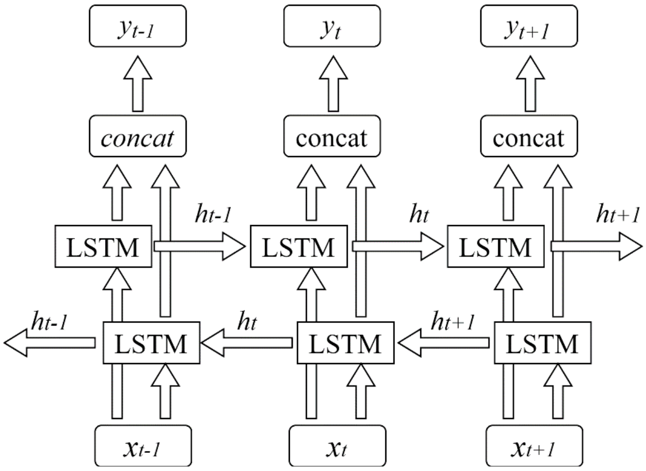

Figure 6. Bi-directional LSTM structure

The structure of bi-directional LSTM used in this study consisted of six layers: (1) the input layer (31 units), (2) the masking layer, (3) the hidden layer (200 units, dropout: 0.2), (4) the hidden layer (200 units, dropout: 0.2), (5) time-distributed layer with linear activation function, and (6) output layer (1 unit). Using the mean squared error as the loss function and adaptive moment estimation optimizer as the optimization function, the batch size was increased to 200-time steps to improve learning efficiency. The initial learning rate was set to 0.0004 and halved every two epochs for a total of six epochs.

Using these trained models, we make predictions on the test data and verify their accuracy. The actual and predicted time historical data were quantitatively compared using CORA [11].

RESULTS

Tables 1 and 2 show the CORA evaluation of the prediction results from LSTM and bidirectional LSTM. The horizontal axis of the table indicates the predicted brain region, and the vertical axis indicates the type of test. The prediction accuracy was excellent (CORA>0.94) for the left and right cerebrum and good (0.8<CORA≤0.94) for the cerebellum and brainstem. Comparing the accuracy of the LSTM and bidirectional LSTM, the latter was found to be more accurate.

Figures 7–10 show examples of the results of the FEA and the LSTM predictions for the left cerebrum principal strain waveforms in each test configuration. For the example of the occipital impact test shown in Figure 7, the waveform predicted by LSTM accurately captured the first peak and accurately predicted the subsequent decay. For the frontal sled test example shown in Figure 8, three small peaks appeared, the first and second peaks were accurately predicted, and the third peak was highly predicted. The vehicle crash test example in Figure 9 shows large peaks at 100 m and 120 m and a small peak at 230 m. The first and second peaks were accurately predicted, while the third small peak was highly predicted.

Table 1
Averaged CORA value of prediction result by LSTM

	Cerebellum	Stem	Cerebrum R	Cerebrum L
Occipital head impact test (*n*=125)	0.952±0.065	0.958±0.053	0.973±0.030	0.970±0.033
Frontal sled test (*n*=7)	0.911±0.091	0.920±0.063	0.935±0.025	0.946±0.018
Vehicle crash test (*n*=35)	0.872±0.072	0.876±0.048	0.923±0.046	0.921±0.040
Football impact test (*n*=53)	0.831±0.109	0.885±0.066	0.894±0.061	0.891±0.075
Full data (*n*=220)	0.908±0.096	0.926±0.068	0.944±0.054	0.942±0.058

Table 2
Averaged CORA value of prediction result by bi-directional LSTM

	Cerebellum	Stem	Cerebrum R	Cerebrum L
Occipital head impact test (*n*=125)	0.956±0.061	0.963±0.058	0.974±0.033	0.972±0.038
Frontal sled test (*n*=7)	0.901±0.124	0.912±0.055	0.939±0.030	0.956±0.027
Vehicle crash test (*n*=35)	0.873±0.080	0.880±0.055	0.934±0.043	0.936±0.042
Football impact test (*n*=53)	0.826±0.136	0.888±0.071	0.892±0.080	0.898±0.068
Full data (*n*=220)	0.909±0.106	0.930±0.072	0.946±0.060	0.948±0.056

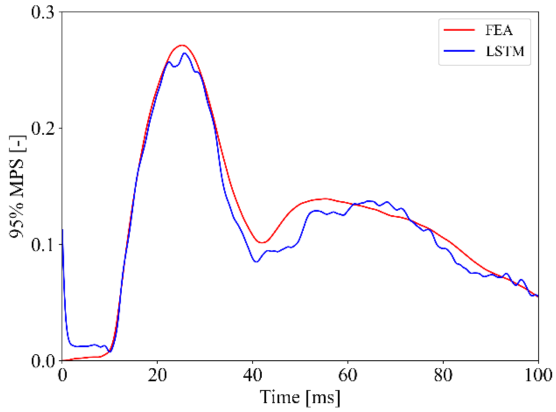

CORA: 0.971

Figure 7. Comparison of waveforms of maximum principal strain between true value (finite element analysis) and predicted value by LSTM in an occipital head impact test case

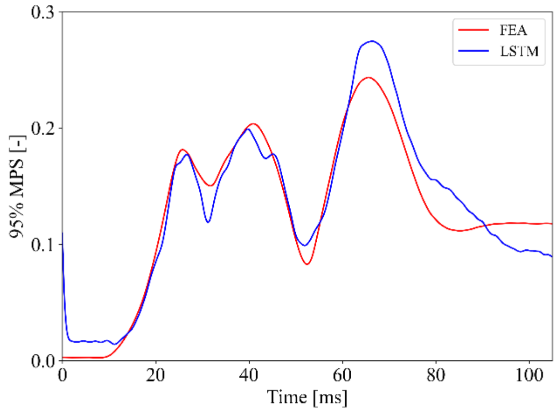

CORA: 0.951

Figure 8. Comparison of waveforms of maximum principal strain between true value (finite element analysis) and predicted value by LSTM in a frontal sled test case

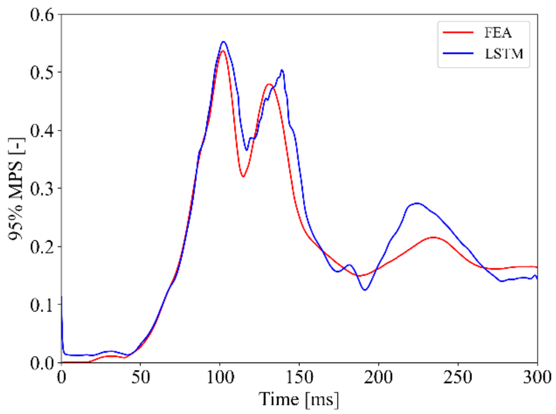

CORA: 0.919

Figure 9. Comparison of waveforms of maximum principal strain between true value (finite element analysis) and predicted value by LSTM in a vehicle crash test case

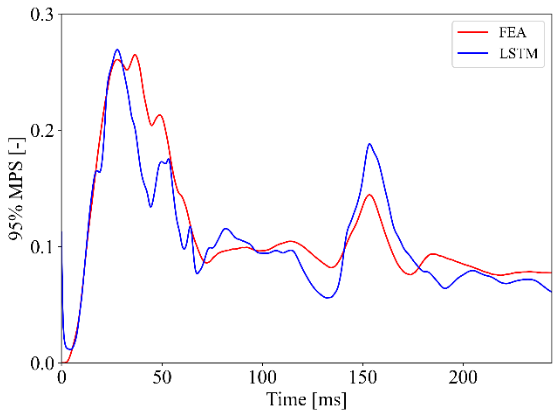

CORA: 0.890

Figure 10. Comparison of waveforms of maximum principal strain between true value (finite element analysis) and predicted value by LSTM in a reconstruction test case of American football

DISCUSSION

Prediction Accuracy of LSTM and Bi-directional LSTM

In Table 2, the bidirectional LSTM yielded a slightly higher prediction accuracy than LSTM. Bi-directional LSTM is mainly used in fields such as natural language processing because it can use the information after a certain point in time when predicting series data. Because the series data used in this study are physical phenomena, future inputs and states did not effectively predict the current outputs and thus did not significantly improve the accuracy.

Prediction Accuracy by Parts of the Brain

As shown in Table 2, the CORA of the right and left cerebrum were larger than those of the cerebellum and brainstem. This was mainly because of the difference in the magnitude of the 95% MPS for each region. The average maximum values of the principal brain strain in the study data are listed in Table 3. The brain strains in the cerebellum and brainstem were small; therefore, the difference in peak values from the brain strain after the impact was small. Therefore, the learning of the brain strain waveform performed poorly.

Table 3
The maximum value of 95 percentile MPS

	cerebellum	stem	cerebrum R	cerebrum L
Averaged max value of MPS	0.107	0.170	0.277	0.271

Prediction Accuracy for Each Head Impact Type

According to the evaluation of each test by CORA shown in Table 2, the prediction accuracy of the waveforms was higher for the occipital impact test, vehicle crash test, frontal sled test, and reconstruction of the football accident. Figures 11 and 12 show the mean and standard deviation of the angular velocity for the occipital head impact tests and reconstruction tests of American football. The head impact tests are characterized by a significant change in angular velocity around the *y*-axis and a small change in angular velocity around the *x*-axis immediately after impact. However, the angular velocity waveforms in the reconstruction tests of American football are widely distributed along the *x*, *y,* and *z* axes. This is because the reconstruction tests of American football cases include head-impact conditions from various directions. Therefore, the prediction accuracy was low because there were few learning opportunities for input waveforms with similar characteristics in the American football cases dataset. The frontal sled test performed poorly because, for the football head impact tests, the number of datasets for the frontal sled test was small, and there were few learning opportunities for impacts with similar characteristics. However, the prediction accuracy did not deteriorate significantly because the dataset of the FRB vehicle crash test and occipital impact tests, which include similar head behavior, were also trained.

Afterward, the prediction errors of the waveforms are discussed for specific examples of the predicted waveforms for each head impact condition, as shown in Figures 7–10. First, the triaxial angular velocity waveforms used as inputs in the prediction are shown in Figures 13 and 14. When predicting the multimodal brain strain waveforms for any collision type, the prediction accuracies of the second and subsequent peaks were slightly less accurate than those of the first peak: the peaks were at 65 m in the frontal sled test (Figure 8), at 130 and 230 m in the vehicle crash test (Figure 9), and 150 m in the reconstruction test case of American football (Figure 10). The multimodal brain strain waveform is caused by head rebound behavior, in which the head rotates in the opposite direction of the initial impact owing to a collision with an airbag. It was difficult to predict changes in brain strain because of this behavior from angular velocity alone because the angular velocity at 70 ms in the frontal sled test (Figure 13) and 130 ms in the vehicle crash test (Figure 14) was small. However, using the features of angular velocity change created by feature engineering, we could incorporate longer-term brain strain changes into the prediction, and the prediction accuracy was improved. Because over half of the current dataset consists of data from occipital impact tests without rebound behavior, further improvement would be expected by expanding the dataset to include rebound behavior or by considering features that can better reflect head rebound behavior.

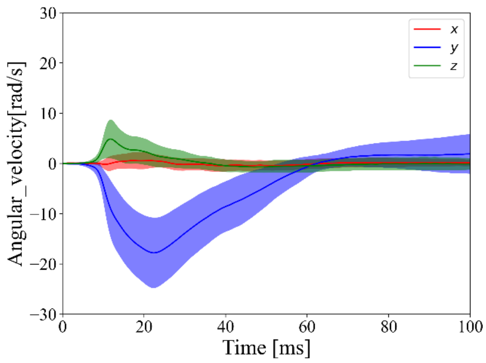

Figure 11. Angular velocity of occipital head impact tests

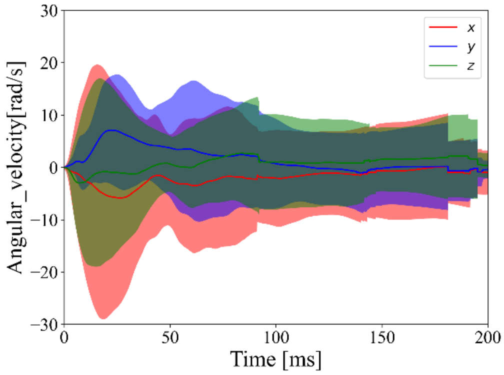

Figure 12. Angular velocity of reconstruction tests of American football

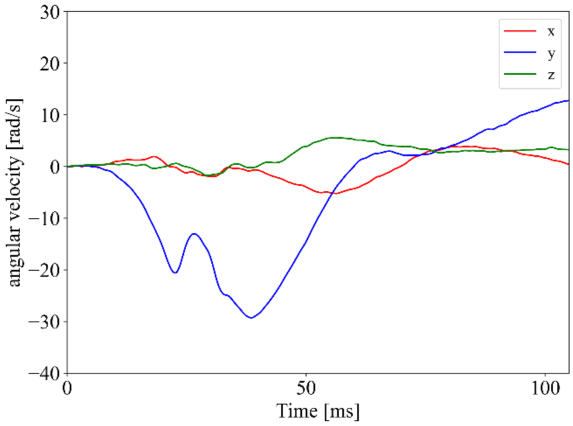

Figure 13. Angular velocity input of frontal sled test

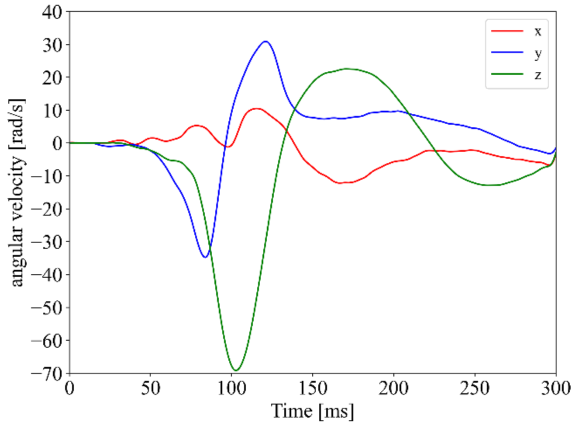

Figure 14. Angular velocity input of vehicle crash test

CONCLUSION

This study proposed a fast and simple method for predicting brain strain waveforms as an alternative to FEA, using LSTM and bidirectional LSTM, which are deep learning methods that can predict time-series waveforms. FEAs were performed on four types of head impact: occipital head impact tests, frontal sled tests, vehicle crash tests, and a reconstruction test of American football. Prediction models of brain strain waveforms using LSTM or bidirectional LSTM were constructed and evaluated. The results indicated that the LSTM model accurately predicted the brain strain waveforms.

REFERENCES

[1] National Police agency,　Traffic accident information, (2021). (in Japanese)

[2] S. Wu, W. Zhao, K. Ghazi, and S. Ji, Convolutional Neural Network for Efficient Estimation of Regional Brain Strains. Scientific Reports, 9(17326):1-11. (2019).

[3] H. Yamamoto, Y. Miyazaki, S. Awamori, A. Kokeguchi, I. Amamori, K. Yoshii, Development of a Method to Measure Intracranial Brain Motion of a Novel Anthropometric Test Dummy Head using 6DOF Sensors, Student Research Symposium of AAAM2020 (2020)

[4] Y. Miyazaki, A. Railkar, S Awamori, A Kokeguchi, I Amamori, M Katagiri, K Yoshii, Intracranial Brain Motion Measurement in Frontal Sled Tests by Using a New Anthropometric Test Dummy Head Capable of Direct Brain motion Evaluation and Visualization, Proceedings of IRCOBI conference, IRC-17-45 (2017)

[5] NHTSA, NHTSA Vehicle Crash Test Database, https://www-nrd.nhtsa.dot.gov/database/veh/veh.htm
[6] E. J. Pellman, D. C. Viano, A. M. Tucker, I.R. Casson, & J. F. Waeckerle, Concussion in Professional Football: Reconstruction of Game Impacts and Injuries. Neurosurgery 53, 799-814(2003).
[7] E. J. Sanchez, et al. A reanalysis of football impact reconstructions for head kinematics and finite element modeling. Clin. Biomech. (2018).
[8] F. Gers, J. Schmidhuber, and F. Cummins, Learning to Forget: Continural Prediction with LSTM, Neural Computation 12,2451-2471, (2000).
[9] S. Hochreiter and J. Schmidhuber, Long Short-Term Memory, Neural Computation, 9(8): 1735-1780, (1997).
[10] Graves, A., Schmid huber, J.: Framewise Phoneme Classification with Bi-directional LSTM and Other Neural Network Architectures. Neural Networks 18(5), 602–610(2005).
[11] Gehre, C., Gades, H. & Wernicke, P. Objective Rating of Signals Using Test and Simulation Responses. In Enhanced Safety of Vehicles (2009)